Journal of Physics: Conference Series **458** (2013) 012011 doi:10.1088/1742-6596/458/1/012011

Quarkonium Results in PbPb Collisions at CMS

M Calderón de la Barca Sánchez[1], for the CMS Collaboration

[1] Physics Department, UC Davis. One Shields Avenue, Davis CA 95616, USA

E-mail: mcalderon@ucdavis.edu

Abstract. We summarize the results from the study of charmonium and bottomonium via the dimuon decay channel in PbPb collisions with the CMS experiment. We discuss the observation of sequential suppression of the Υ states. We present preliminary results of prompt J/ψ and ψ' production, as well as of non-prompt J/ψ's coming from the weak decay of b-quarks. This latter measurement is sensitive to b-quark energy loss. We discuss the results and compare to model predictions.

1. Introduction

Quarkonium suppression in a hot colored medium is a longstanding signature of quark-gluon plasma (QGP) formation. It is expected that suppression will arise due to two main effects. The first mechanism proposed was color Debye screening [1]. In the vacuum, a heavy quark-antiquark bound state, such as charmonium or bottomonium, are kept together by the QCD color field. Simulations of QCD on the lattice show that the color fields take the form of a color-flux tube, which gives rise to an approximately linear potential. Since the quarks are massive and move at low velocities, one can use the framework of non-relativistic QCD. The spectroscopy of charmonia and bottomonia can be obtained this way. In a hot QCD medium, the expectation is that the additional color charges around the heavy quark-antiquark pair will produce color fields which screen the potential between them. The Debye screening radius depends on the temperature, and this then leads to a suppression of excited quarkonium states according to their average radius. This picture has been augmented with recent studies which find that there is also a broadening of the quarkonium spectral functions due to the interaction of soft gluons in the QGP medium with the quarkonium state. The effects of gluo-dissociation and Landau damping can be encapsulated in the quark-antiquark potential as an imaginary part, with the real part governing the screening behavior. For a review of this subject, see Ref. [2]. More recently, attempts to calculate the potential directly in the lattice have been done, including the real and imaginary parts, i.e. screening and Landau damping/gluo-dissociation. These studies motivate the continued study of quarkonia in relativistic heavy ion collisions, since an observation of suppression could then be connected to the properties studied in the lattice. In this way, we could estimate the temperature reached in the medium. Furthermore, a suppression due to hot nuclear matter effects in the bottomonium case would be a clean signature of deconfinement. (The picture is complicated in the case of charmonium due to the competing effect of recombination, which is negligible for the case of bottomonium due to the small bottom cross section even at LHC energies.) In this paper, we present a summary of some key results from the CMS in the field of quarkonium studies in relativistic heavy ion collisions. The manuscript is organized as follows: We briefly describe the detector and analysis preliminaries, then we discuss the results from prompt charmonium. Next,

we present the results from non-prompt J/ψ which originate mainly from B meson decays. We then discuss bottomonium measurements, followed by a summary of our findings.

2. CMS Detector and Data

A detailed description of the CMS detector can be found in Ref. [3]. The main detectors used in this analysis are the Muon detectors and the silicon tracker. The solenoidal superconducting magnet of 6m internal diameter provides a $B = 3.8$ T field. It houses the silicon pixel and silicon strip tracker, as well as electromagnetic and hadronic calorimeters. The tracker can measure charged tracks in the kinematic range $|\eta| < 2.5$. Muons are detected via drift tubes, cathode strip chambers and resistive plate chambers in the range $|\eta| < 2.4$. The granularity of the tracker working in tandem with the strong bending B field allow for measuring muon transverse momenta (p_T) with resolution in the range $1 - 2\%$ for the analyses presented here. The muons need a minimum total momentum in the range $3 - 5$ GeV/c to reach the muon stations. This places limits on the acceptance of J/ψ mesons. For mid-rapidity, we can measure J/ψ in the range $p_T > 6.5$ GeV/c, while at forward rapidity, we can measure it down to $p_T > 3$ GeV/c. For the Υ mesons, the higher mass is transformed to a higher muon momentum in the decay process, allowing us to measure Υ mesons down to $p_T > 0$ for all rapidity.

To estimate the collision centrality, we measure the transverse energy (E_T) in a hadron calorimeter placed in the forward region (HF, $2.9 < |\eta| < 5.2$). We use a Glauber model to simulate the $N_{\rm part}$ distributions based on fits to the HF E_T measurements, as described in Ref. [4].

3. J/ψ Production

In the invariant mass spectrum of dimuons, CMS can measure J/ψ mesons and estimate the prompt and non-prompt contributions [5]. We distinguish these two categories as follows. The prompt component originates from directly produced J/ψ plus those which arise from the secondary decays of charmonium excited states, such as the ψ' and χ_c. These excited state transitions are sufficiently fast that the muons we observe are indistinguishable from primary muons. The non-prompt component arises mainly from the decay of beauty hadrons, chiefly B mesons. These weak decays are longer lived, with lifetimes of order $c\tau \approx 490\mu$m (for B^+). By reconstructing the invariant mass, the position of the secondary vertex in the transverse plane L_{xy}, and the pair p_T, we can do a simultaneous fit of the invariant mass spectrum together with the pseudo-decay length $\ell_{J/\psi} = L_{xy} m_{J/\psi}/p_T$. This allows us to estimate the contributions of prompt and non-prompt J/ψ separately.

3.1. Prompt J/ψ

We have measured the production of prompt J/ψ in both PbPb and pp collisions at $\sqrt{s}$=2.76 TeV. To quantify the modifications observed in going from pp to PbPb, we scale the yields measured in pp using the Glauber model from Ref. [4] and use this to normalize the PbPb measurements, constructing the nuclear modification factor R_{AA}. Figure 1 shows R_{AA} of prompt J/ψas a function of $N_{\rm part}$, p_T, and y.

For the top 5% most central collisions in the kinematic range $p_T > 6.5$ GeV/c we observe a suppression of a factor of ~ 5. For the centrality-integrated data, we do not observe a significant p_T or rapidity dependence of the suppression in our measured kinematics. Comparing the data to the model calculations from Zhao and Rapp [6], given by the various lines in the left panel of Fig. 1, shows a qualitative agreement with the observed trend of increasing suppression, i.e. decreasing R_{AA}, with increasing $N_{\rm part}$. In this model, for our kinematics, the mechanism responsible for the suppression are the hot nuclear matter effects, screening and gluo-dissociation, discussed previously.

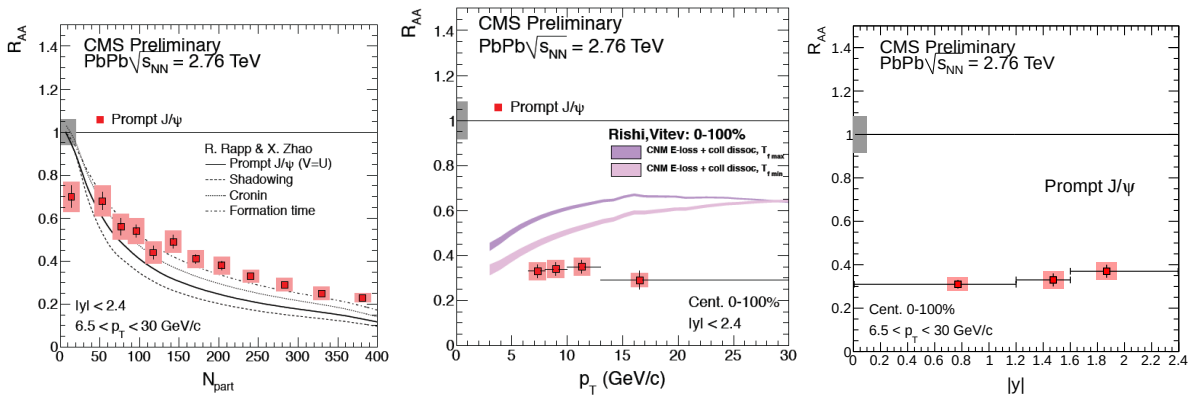

Figure 1. The nuclear modification factor, R_{AA}, for prompt J/ψ as a function of $N_{\rm part}$ (left), p_T(center) and $|y|$ (right). The kinematic range for the measurement is $6.5 < p_T < 30$ GeV/c, and $|y| < 2.4$. The data show a clear suppression with increasing $N_{\rm part}$, but no p_T or y dependence. For discussion of the model comparisons, see text.

We see no evidence for a contribution from statistical recombination, which is expected to contribute to the J/ψ yield at lower p_T. In contrast, a model from Sharma and Vitev [7] based on cold-nuclear-matter energy loss plus collisional dissociation of J/ψ mesons expects less suppression with increasing p_T, in disagreement with the observed level of suppression that remains constant in our measurement region.

We have also measured the nuclear modification factor for the ψ' meson. We find that in the kinematic region $p_T > 6.5$ GeV/c and $|y| < 1.6$ the ψ' is suppressed much more than the J/ψ. Our preliminary result in this kinematic region integrated over all centralities is $R_{AA}(\psi(2S)) = 0.11 \pm 0.03$ (stat.) $\pm$ 0.02(syst.) $\pm$ 0.02(pp). In the forward rapidity region, $1.6 < |y| < 2.4$ and lower p_T (down to 3 GeV/c) we find an enhancement of the ψ'. However, the current statistics from the pp measurement hinder the statistical significance of the forward y measurement. With pp data from 2013 this situation will be ameliorated.

3.2. Non-prompt J/ψ production

The non-prompt contribution to the inclusive J/ψ yield was also extracted from the PbPb and pp data. The nuclear modification factor R_{AA} is shown in Figure 2. The dependence of R_{AA} on centrality, p_T and y is shown in the left, middle and right panel, respectively.

We find an increasing suppression for non-prompt J/ψ with increasing $N_{\rm part}$. The suppression reaches a factor 2.5 ($R_{AA} \approx 0.4$) for the top 5% most central events. When integrated over centrality, there is a hint of increasing suppression with increasing p_T or y. As mentioned earlier, the non-prompt J/ψ production is dominated by the decays of B mesons. Therefore, suppression of the non-prompt J/ψ yield is expected to be a sensitive probe to energy loss of b-quarks. Due to the large mass of the b ($m_b \sim 4.2$ GeV/c^2), the radiative energy loss of b quarks is expected to be suppressed, when compared to light parton gluon Bremsstrahlung, at forward angles of order $\theta \lesssim m/E$, where θ is the angle between the radiated gluon and the direction of the propagating quark, m is the quark mass of the heavy quark, and E its Energy. Measurements of non-photonic electron R_{AA} at RHIC indicated that, in addition to radiative energy loss, b quark production also had a significant modification due to collisional energy loss. In the comparison of the R_{AA} vs. p_T data to model calculations, we find that the model from Vitev, based on Ref. [8], with only radiative energy loss does not give enough suppression to be consistent with our measurement (light blue band). The addition of collisional energy loss (dark blue) is in much better quantitative agreement with our data. A calculation

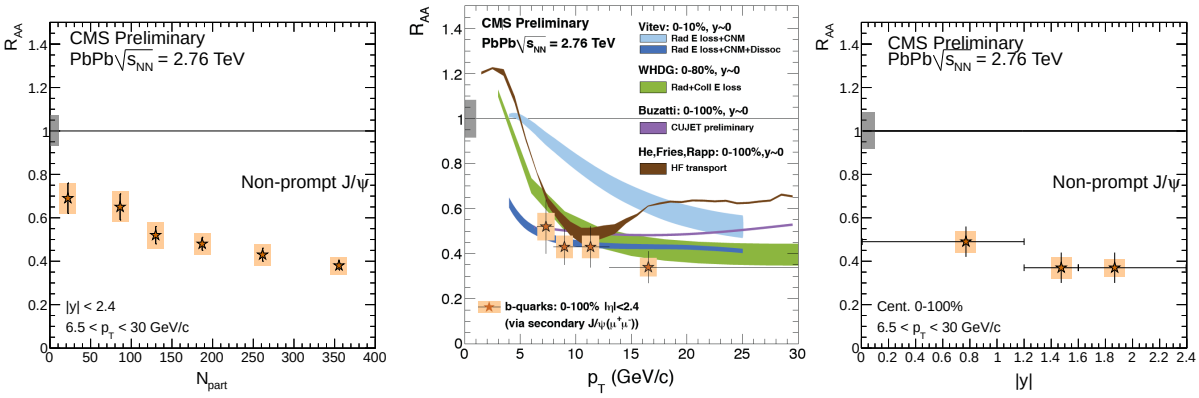

Figure 2. The nuclear modification factor, R_{AA}, for non-prompt J/ψ, which mainly come from B meson decays, as a function of $N_{\rm part}$ (left), p_T(center) and $|y|$ (right). The kinematic range for the measurement is $6.5 < p_T < 30$ GeV/c, and $|y| < 2.4$. For discussion of the experiment and model comparisons, see text.

in the energy-loss framework developed by Wicks, Horowitz, Djordjevic and Gyulassy, including both the radiative and collisional energy-loss mechanisms, is also shown. The framework was developed for comparing to RHIC data, and is based on pQCD weak-coupling and AdS/CFT strong-coupling drag energy loss models [9]. The model parameters were set at RHIC and then kept constant to predict the R_{AA} at LHC (green band). We see that this model is in good quantitative agreement with our data. Note that our data are given in terms of the p_T of the measured J/ψ while the calculations are given in terms of the p_T of the B meson, which is always higher than the daughter J/ψ p_T. Therefore, one would expect a slight shift of the model curves to lower p_T to account for this. We also compared our data to calculations from the CUJET model [10] and He et al. [11], which also are in good agreement with our data at low p_T. The energy-loss model from He et al., which is based on a heavy-quark diffusion and hadronization picture, expects less suppression with increasing p_T which is in disagreement with our highest measured p_T R_{AA}.

4. Bottomonium

We have measured the Υ family in both the pp and PbPb collision systems. Figure 3 shows the invariant mass of dimuon pairs measured in pp (left) and PbPb (center and right). The excellent resolution of the CMS detector for muons allows a clear separation of all 3 states [12]. The data are fit in order to extract various parameters of interest, in particular the raw (not acceptance corrected) single ratios $\Upsilon(nS)/\Upsilon(1S)$ in both collision systems and the double ratio of these raw single ratios between the PbPb and pp system $(\Upsilon(nS)/\Upsilon(1S))_{\rm PbPb}/(\Upsilon(nS)/\Upsilon(1S))_{pp}$. The raw single ratios cancel uncertainties arising from mechanisms which affect the excited states and the ground state in the same way. An example of such a mechanism is the uncertainty arising from the parton distribution functions. For Υ production, the dominant production channel is gluon-gluon fusion, hence the gluon PDF is the one that plays the most important role. Since this PDF enters in the same way in the production of the bottomonium final state, namely in the initial state entrance channel, any modifications will affect the ground state and the excited states in the same way, thus they will cancel in the single ratio. An important experimental effect which does not cancel in the raw single ratio is a difference in the acceptance for excited states compared to the ground state. This difference in acceptance arises from the fact that the muons chosen for the analysis must satisfy ${p_T}^{\mu} > 4$ GeV/c. Since we look for two muons in order to reconstruct the Υ mesons, and the p_T threshold is close to half of the Υ mass, it is appreciably

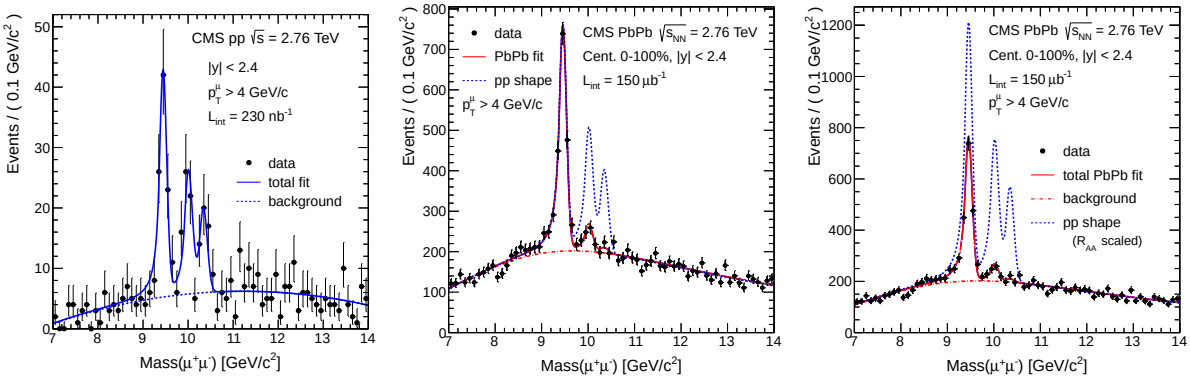

Figure 3. The invariant mass distribution of dimuons. The *pp* data are shown in the left panel. The center and right panel both show the PbPb data. The *pp* and PbPb data are fit, with the result shown on the plot. The *pp* fit is shown in the center and right panels to graphically illustrate the double ratio $(\Upsilon(nS)/\Upsilon(1S))_{\rm PbPb}/(\Upsilon(nS)/\Upsilon(1S))_{pp}$ (center) and the nuclear modification factor scaling R_{AA} (right). See text for details.

easier for a state at higher mass to have its muon daughters satisfy the p_T threshold compared to a lower-mass Υ meson. This acceptance effect will cancel in the double ratio between PbPb and *pp*. This makes the double ratio a very robust observable for quantifying modifications of the excited states with a very small systematic uncertainty. This is illustrated graphically in the center panel of Fig. 3. The shape of the invariant mass fit to the Υ states in the *pp* collision system is overlaid on the PbPb data. In the single ratio, the Υ(1S) yield is the reference, and in the double ratio the PbPb and pp ratios are then compared. By construction, the double ratio for the 1S is 1, so the 1S peaks in PbPb and *pp* have the same height in the figure. The interesting observation then is to see what happens to the excited states. If the excited-to-ground state ratio in PbPb was the same as in *pp*, the blue dotted line (*pp* shape) would also match the PbPb data for the excited states. Clearly it does not. Therefore, we conclude that the excited states are modified in PbPb. Furthermore, we surmise that this modification is not arising from nuclear PDFs, because they would affect the excited states in the same way as the ground state. It remains to be seen whether this is strictly a hot nuclear matter effect by doing this measurement in the pPb collision system.

In the right panel, we illustrate graphically a different scaling. To compare absolute yields for each state between *pp* and PbPb, we again use a Glauber model to estimate the nuclear overlap and the number of collisions, $N_{\rm coll}$. Using this information, we scale the measured yields in *pp* and compare them directly to the data. The blue dotted line in the right panel shows this expected *pp* yield, which is the denominator in the construction of the nuclear modification factor R_{AA}. One can see in this way that the inclusive yield for all Υ states in PbPb collisions shows suppression compared to the binary-scaled *pp* yield.

The results for the nuclear modification factor, R_{AA} of Υ mesons are shown in Fig. 4. With the 150 μb^{-1} of integrated luminosity sampled in 2011, we are able to split the Υ(1S) and Υ(2S) data into 7 centrality bins. The Υ(1S) data are shown as the red filled squares in the left panel of Fig. 4, and as the green diamonds in the center and right panels. The Υ(2S) data are shown as the green filled circles in the left panel, and as the blue filled circles in the center and right panels. The small panel to the right of the left panel shows the centrality integrated R_{AA} values:

- $R_{AA}(\Upsilon(1S)) = 0.56 \pm 0.08(\text{stat.}) \pm 0.07(\text{syst.})$
- $R_{AA}(\Upsilon(2S)) = 0.12 \pm 0.04(\text{stat.}) \pm 0.02(\text{syst.})$
- $R_{AA}(\Upsilon(3S)) < 0.1$ at 95% C.L.

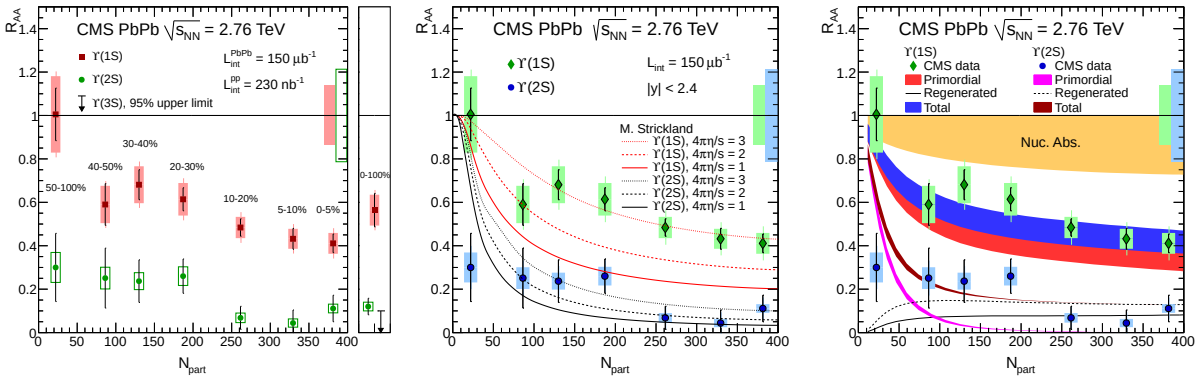

Figure 4. The nuclear modification factor, R_{AA}, for Υ mesons as a function of $N_{\rm part}$. (Left) The red filled squares show our results for Υ(1S) and the green filled circles are for Υ(2S). The small panel to the right of this figure shows the centrality integrated values. The upper limit for the Υ(3S) is shown as the arrow in this panel. (Center) The same data for the Υ(1S) and Υ(2S) are shown in as green diamonds and blue circles, respectively. The data are compared to a model calculation from Ref. [15]. (Right) The Υ data are the same as in the center panel. The data are compared to a model calculation from Ref. [16]. See text for details.

This is the first measurement of Υ(2S) R_{AA}. In addition, the R_{AA} values we observe are ordered in the expected way: smaller R_{AA} for the states with the smaller binding energy and larger radius.

In studying the data as a function of centrality, we find that the Υ(1S) and Υ(2S) suppression increases with $N_{\rm part}$. For all the centrality bins, we observe the suppression of the Υ(2S) state to be larger than the suppression of the Υ(1S). In the most peripheral bin, the Υ(1S) nuclear modification factor is consistent with unity, while that for the Υ(2S) remains low. However, it should be noted that this bin includes a wide impact parameter range (50-100% of the total cross section), and it is expected that most of the events where an Υ will be produced will be biased towards larger $N_{\rm coll}$ and hence smaller impact parameter.

Our measurements are of inclusive production of Υ mesons, which include both the directly produced Υ mesons and those which are the daughters of excited states. For example, the χ_b meson can decay via $\chi_b \to \Upsilon(1S)+\gamma$. The χ_b is less tightly bound and has a larger average radius than the Υ(1S). If the χ_b states are suppressed in the QGP, this will reduce the contribution from one of the sources of Υ(1S) and will lead to a suppression even if the directly produced Υ(1S) mesons do not melt in the QGP or are otherwise modified. This contribution from feed-down of higher excited states has been measured by CDF at lower $\sqrt{s}$ and by LHCb at higher $\sqrt{s}$ [13, 14]. Both experiments find that the feed-down contribution to the Υ(1S) yield is $\approx 50\%$. However, this contribution has only been measured at high p_T. If the contribution is the same at lower p_T, a suppression of all the excited states down to $R_{AA} = 0$ but with no suppression of Υ(1S) would result in $R_{AA} \approx 0.5$ for the Υ(1S). Under this hypothesis, our data for the most central events for the Υ(1S) is consistent with the suppression affecting only the excited states. This scenario illustrates the importance of including the effects of feed-down when making comparisons to our inclusive measurements.

Two such comparisons are shown in the center and right panels of Fig. 4. In the center panel, we compare our results to a model calculation by Strickland and Bazow [15]. In this model, the heavy-quark potential is taken to be the heavy-quark internal energy as calculated in the lattice. (The calculation was also done with the free energy and found to be inconsistent with our data. The free-energy calculation is not shown.) In addition, the model also includes the imaginary

part of the potential (the Landau damping and gluo-dissociation effects discussed previously). These ingredients naturally lead to sequential melting. In addition to including the effects of feed-down, under the assumption that the contribution from excited states is as measured by CDF in the entire p_T range, the model includes a dynamical expansion using the framework of anisotropic hydrodynamics. The model was run under three different choices for the value of the shear viscosity to entropy ratio, $4\pi\eta/S$ =1, 2, and 3. For each of these choices, the initial temperature was also adjusted in order to match the existing measurements of multiplicity. The temperatures used were in the range $552 < T_0 < 580$ MeV. The highest temperature corresponds to the lowest shear viscosity to entropy ratio, and these are shown as the solid lines in Fig. 4, center. The red line is for the Υ(1S) and the blue line is for the Υ(2S). The Υ(1S) data seems to be best described by the calculation with the lowest temperature and highest shear viscosity to entropy ratio in this model. There is some tension to describe the Υ(2S) data with this same set of parameters, although with the statistical uncertainty for the Υ(2S) data none of the choices can be ruled out to more than 2σ.

The right panel of Fig. 4 shows a comparison to a model calculation from Emerick et al. [16]. The authors of this calculation considered two scenarios. In one scenario, the binding energy of the states was varied with temperature, such that at large temperature the binding was small. This was dubbed the "Weak-Binding Scenario". The second scenario assumed that there is no variation of the binding energy with temperature. The bound states remain with the same masses and binding energies as in the vacuum throughout their dynamical evolution in the QGP. This was called the "Strong-Binding Scenario". As an example of the differences, the bottomonium spectral function is much wider in the Weak-Binding compared to the Strong-Binding scenario. In comparing this to lattice data using the so-called euclidean correlator, which is the integral of the spectral function over some kernel, it was found that the Strong-Binding scenario results in a better agreement with the finding that the correlators do not change very much with temperature. This has been taken as a strong motivation for preferring the Strong-Binding scenario. In this model, both Landau damping and gluo-dissociation become the leading break-up mechanisms, with the former being more important for weakly bound states and the latter for states with large binding energy. The dynamical evolution is done in the framework of kinetic theory. The primordial suppression, including feed-down contributions, is shown as the red band in Fig. 4, right, for the Υ(1S). For the Υ(2S) it is shown as the magenta band. In this model, the primordial Υ(2S) yield is completely suppressed in the most central collisions. This model also includes a parameterization of cold-nuclear matter effects, based on preliminary results from d+Au collisions from STAR [17]. In addition, the model incorporates a contribution from regeneration of Υ mesons via the coalescence of uncorrelated b-$\bar{b}$ pairs produced in the same event. The solid black line shows this contribution for the Υ(1S), and the dotted black line shows the corresponding contribution for the Υ(2S). The total nuclear modification factor, including all contributions, is shown as the blue band for the Υ(1S) and as a brown band for the Υ(2S). Given the small b-$\bar{b}$ cross section, the total suppression is not too different from the primordial result in this model. There is still a large uncertainty in the nuclear absorption, underlining the need for results from d+Au and p+Pb collisions. In this model the initial temperature reached in the QGP is $T_0 \approx 610$ MeV.

5. Summary

We presented the results from Quarkonia production measured by CMS in the heavy ion collision environment. We have measured charmonia at high-p_T in the mid-rapidity region. We found that the J/ψ mesons are suppressed, and the ψ' mesons at mid-rapidity are suppressed more than the J/ψ. This pattern is as expected from the sequential melting picture. The non-prompt J/ψ measurement allows us to study b-quark energy loss. Calculations incorporating radiative and collisional energy loss are consistent with our preliminary measurements. In the

bottomonium sector, we also observe a clear ordering of the suppression of the three Υ states with binding energy. A plot summarizing the observed nuclear modification factors for all the quarkonia states discussed in this manuscript is shown in Fig. 5. The horizontal axis indicates

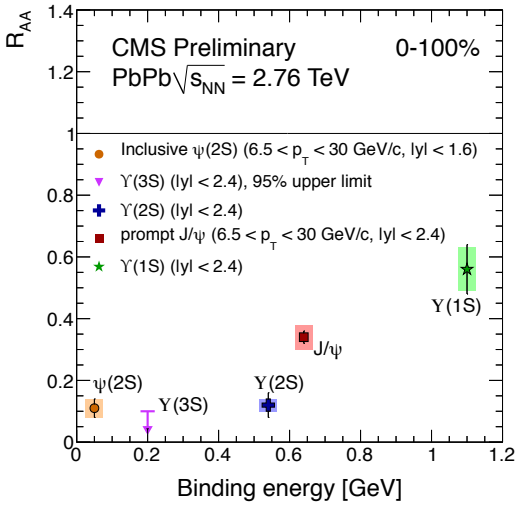

Figure 5. Nuclear modification factor, R_{AA}, for the quarkonia measured by CMS in heavy ion collisions shown as a function of the binding energy of the state. A sequential suppression pattern is observed. See text for details.

the binding energy of the given quarkonium state. The ψ' is the state with the smallest binding energy, and the Υ(1S) is the most tightly-bound state. The binding energy is simply taken to be the vacuum binding energy, i.e. the mass difference between the quarkonium state and the open heavy-flavor continuum, given by twice the mass of the D meson for the charmonium states and twice the mass of the B meson for the bottomonium family. We observe a pattern of sequential suppression of quarkonium states. This pattern is consistent with the expectation that quarkonia will melt in a hot quark-gluon plasma, with the least tightly bound states melting first. The temperatures reached in the plasma in the two model calculations used for comparison to our data are in the range 550 – 610 MeV. We look forward to measurements of quarkonia in p+Pb collisions, which will be important to distinguish cold and hot nuclear matter effects.

References

[1] T. Matsui and H. Satz, Phys. Lett. B **178**, 416 (1986)
[2] N. Brambilla, S. Eidelman, B. K. Heltsley, R. Vogt, G. T. Bodwin, E. Eichten, A. D. Frawley and A. B. Meyer *et al.*, Eur. Phys. J. C **71**, 1534 (2011) [arXiv:1010.5827 [hep-ph]].
[3] S. Chatrchyan *et al.* [CMS Collaboration], JINST **3**, S08004 (2008).
[4] S. Chatrchyan *et al.* [CMS Collaboration], JHEP **1108**, 141 (2011) [arXiv:1107.4800 [nucl-ex]].
[5] CMS Collaboration, J/ψ results from CMS in PbPb collisions with 150μb^{-1} data, PAS HIN-12-014.
[6] X. Zhao and R. Rapp, Nucl. Phys. A **859**, 114 (2011) [arXiv:1102.2194 [hep-ph]].
[7] R. Sharma and I. Vitev, Phys. Rev. C 87, **044905** (2013) [arXiv:1203.0329 [hep-ph]].
[8] I. Vitev, J. Phys. G **35**, 104011 (2008) [arXiv:0806.0003 [hep-ph]].
[9] W. A. Horowitz, AIP Conf. Proc. **1441**, 889 (2012) [arXiv:1108.5876 [hep-ph]].
[10] A. Buzzatti and M. Gyulassy, arXiv:1207.6020 [hep-ph].
[11] M. He, R. J. Fries and R. Rapp, Phys. Rev. C **86**, 014903 (2012) [arXiv:1106.6006 [nucl-th]].
[12] S. Chatrchyan *et al.* [CMS Collaboration], Phys. Rev. Lett. **109**, 222301 (2012) [arXiv:1208.2826 [nucl-ex]].
[13] T. Affolder *et al.* [CDF Collaboration], Phys. Rev. Lett. **84**, 2094 (2000) [hep-ex/9910025].
[14] R. Aaij *et al.* [LHCb Collaboration], JHEP **1211**, 031 (2012) [arXiv:1209.0282 [hep-ex]].
[15] M. Strickland and D. Bazow, Nucl. Phys. A **879**, 25 (2012). [arXiv:1112.2761 [nucl-th]].
[16] A. Emerick, X. Zhao and R. Rapp, Eur. Phys. J. A **48**, 72 (2012) [arXiv:1111.6537 [hep-ph]].
[17] R. Reed [STAR Collaboration], J. Phys. Conf. Ser. **270**, 012026 (2011) [Nucl. Phys. A **855**, 440 (2011)].